Elucidating the mechanical properties of asymmetric membranes by direct derivation of their energetics

Supporting Information

Giacomo Fiorin (1,2) and Lucy R. Forrest (1)
(1) Computational Structural Biology Section, National Institute for Neurological Disorders and Stroke, National Institutes of Health, Bethesda, MD 20894, USA
(2) Theoretical Molecular Biophysics Section, National Heart, Lung and Blood Institute, Bethesda, National Institutes of Health, MD 20894, USA

Table S1. Bilayer bending moduli k_c and tilt moduli k_t derived by fitting the theoretical expression for the curvature energy (eq. 2 in the main text) against the computed bending energy landscapes. Standard errors were computed by dividing the simulated trajectory in five segments.

Lipid type		Area	k_c	k_t
Upper	Lower	asymmetry	(kcal/mol)	(kcal/mol/Å^2)
POPC	POPC	0	21.7 ± 1.0	0.117 ± 0.006
		0.029	26.5 ± 1.2	0.109 ± 0.005
		0.051	24.7 ± 0.5	0.105 ± 0.002
		0.067	23.7 ± 0.8	0.096 ± 0.003
POPC	DOPC	–0.057	24.1 ± 0.5	0.124 ± 0.003
		–0.027	24.8 ± 1.1	0.123 ± 0.005
		0.003	21.0 ± 0.9	0.123 ± 0.005
		0.027	24.6 ± 0.4	0.123 ± 0.002
		0.048	22.6 ± 0.9	0.111 ± 0.005

Table S2. Bilayer parameters derived using the same procedure as in Table S1 while including the contribution of the "softening length" ℓ (Diggins *et al*, JACS **137**:12752-12755, 2015).

Lipid type		Area	k_c	k_t	Softening
Upper	Lower	asymmetry	(kcal/mol)	(kcal/mol/Å^2)	length (Å)
POPC	POPC	0	23.0 ± 1.8	0.124 ± 0.008	13 ± 47
		0.029	28.2 ± 1.4	0.116 ± 0.006	–15 ± 46
		0.051	27.8 ± 2.6	0.118 ± 0.011	12 ± 63
		0.067	23.7 ± 0.9	0.097 ± 0.003	–3 ± 7
POPC	DOPC	–0.057	24.2 ± 0.5	0.125 ± 0.002	10 ± 12
		–0.027	25.1 ± 0.8	0.124 ± 0.004	–15 ± 17
		0.003	21.7 ± 1.1	0.123 ± 0.004	2 ± 4
		0.027	24.7 ± 0.5	0.124 ± 0.002	–5 ± 11
		0.048	22.6 ± 0.9	0.112 ± 0.004	0 ± 1

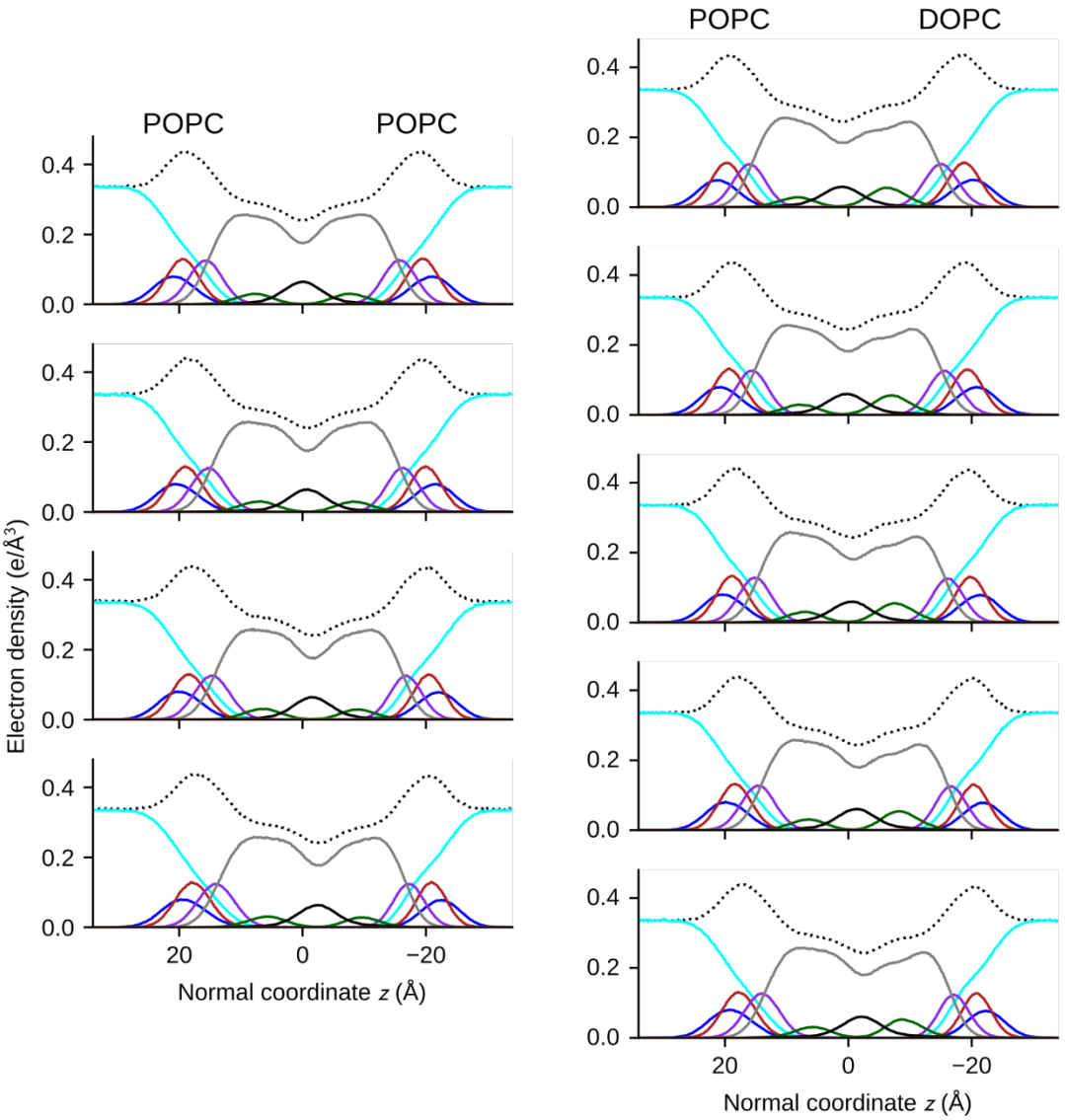

Figure S1. Electron density profiles for POPC/POPC bilayers (left) and compositionally asymmetric POPC/DOPC bilayers (right). Panels are sorted in order of increasing asymmetry from top to bottom. The density profiles of all atoms are shown as dashed lines, alongside partial density profiles for water (cyan), cholines (blue), phosphates (red), glycerols (purple), -CH_2- groups (grey), -CH- groups (green) and terminal -CH_3 groups (black).

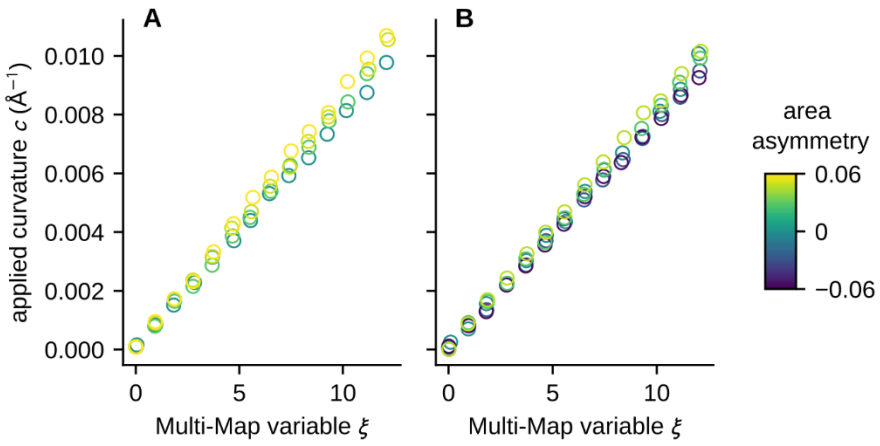

Figure S2. Relationship between the mean value of ξ over the trajectory of each simulation window and the corresponding root-mean-squared curvature c. The latter was computed by extracting the magnitude of sinusoidal deformation from the two-dimensional maps of the bilayer the midplane of each simulation window (see e.g. top rows of Figs. S4 and S5) and evaluating the root-mean-squared curvature of the sinusoidal deformation over the plane. **(A)** Data for the POPC/POPC bilayers; **(B)** data for the POPC/DOPC/bilayers.

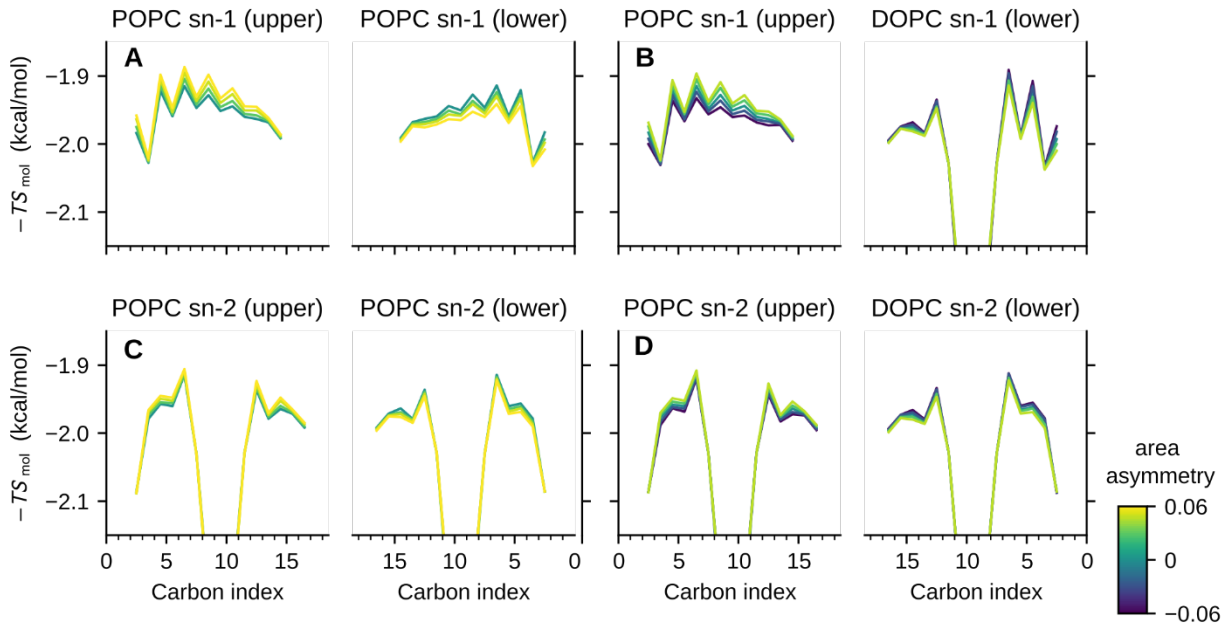

Figure S3. Conformational entropy along the lipid acyl chains, computed from the histograms of each type of torsional angle; values are averaged over all lipid molecules in each leaflet and plotted as a function of the position along each acyl chain. Shown are the values for POPC/POPC bilayers **(A,C)** and in POPC/DOPC bilayers **(B,D)**, distinguished by each acyl chain.

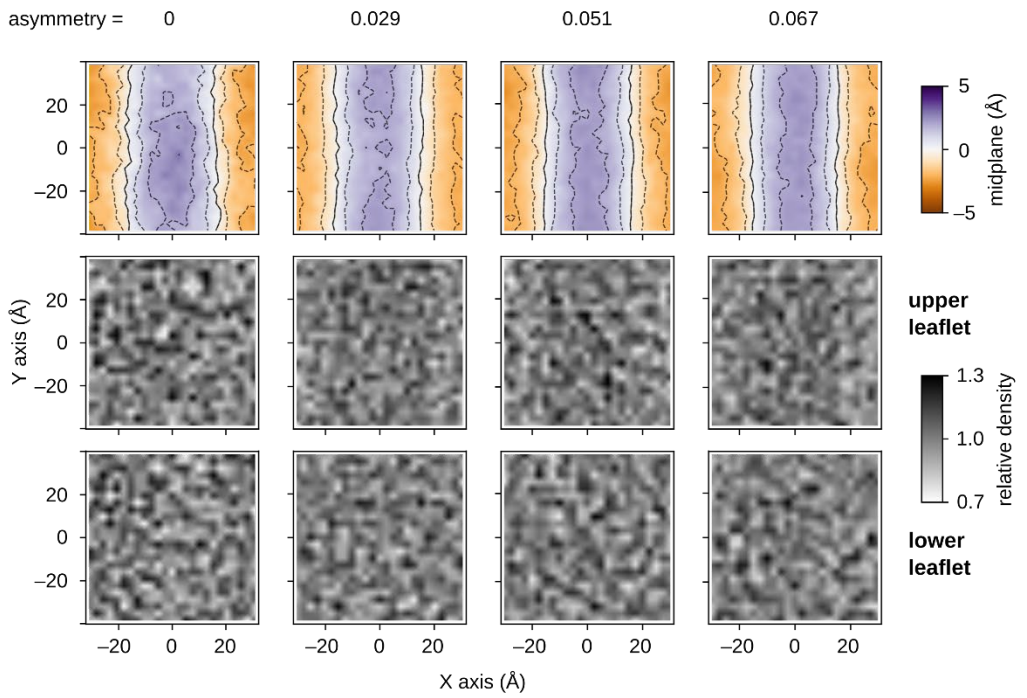

Figure S4. Two-dimensional maps, computed over simulations of deformed POPC/POPC bilayers, of the local position of the bilayer's midplane relative to its mean (top row). Also shown are the variations in local density of the phospholipids relative to the mean for the upper leaflet (middle row) and the lower leaflet (bottom row). Data were computed over the trajectory of the umbrella-sampling simulation window at the highest deformation.

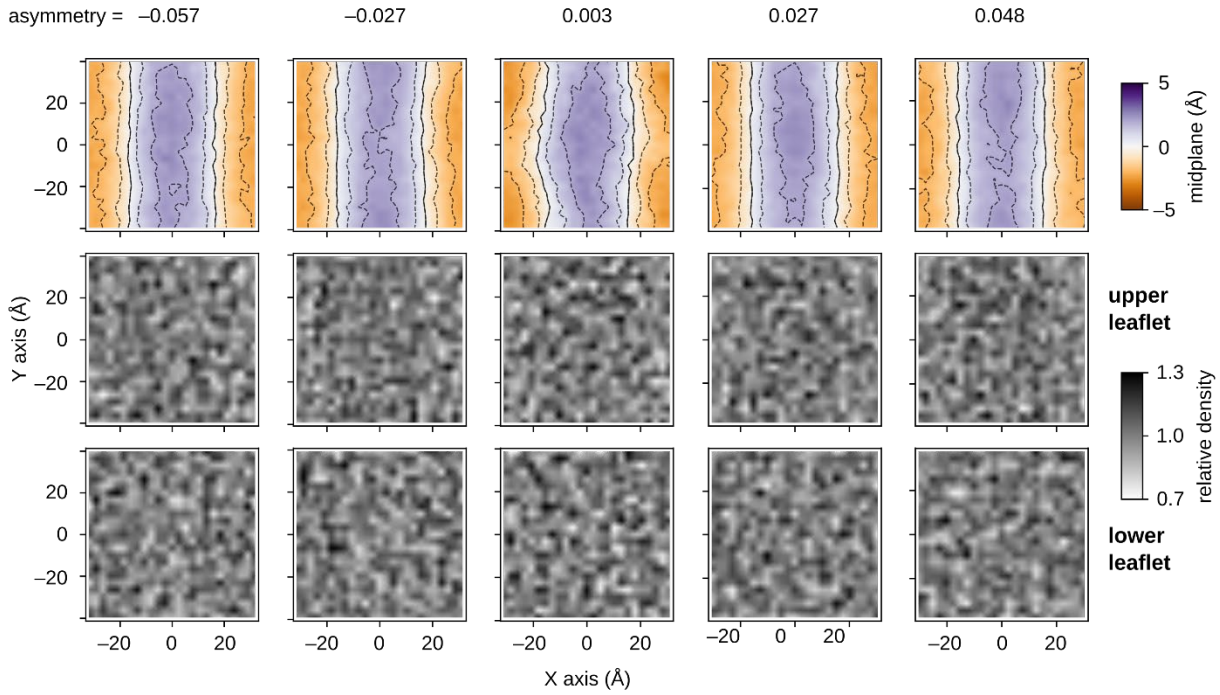

Figure S5. Two-dimensional maps computed over simulations of deformed POPC/DOPC bilayers. See Figure S4 for details.